The Journal of Antibiotics (2019) 72:991–995
https://doi.org/10.1038/s41429-019-0217-5

JARA Japan Antibiotics Research Association
The Society for Actinomycetes Japan

SPECIAL FEATURE: BRIEF COMMUNICATION

Nocardamin glucuronide, a new member of the ferrioxamine siderophores isolated from the ascamycin-producing strain *Streptomyces* sp. 80H647

Julius Adam V. Lopez[1] · Toshihiko Nogawa[1] · Yushi Futamura[1] · Takeshi Shimizu[1] · Hiroyuki Osada[1]

Received: 21 April 2019 / Revised: 4 June 2019 / Accepted: 10 July 2019 / Published online: 8 August 2019
© The Author(s), under exclusive licence to the Japan Antibiotics Research Association 2019

Abstract

A new siderophore glucuronide, nocardamin glucuronide (**1**), was isolated together with nocardamin (**2**) by applying the one strain-many compounds (OSMAC) approach to the ascamycin-producing strain, *Streptomyces* sp. 80H647, and performing multivariate analysis using mass spectral data. Structure elucidation was accomplished by a combination of NMR and MS analyses. The absolute configuration of the glucuronic acid moiety was found to be β-D-GlcA by hydrolysis using β-glucuronidase, subsequent derivatization of the hydrolysate, and comparison with standards. The siderophore activity of **1** was evaluated through the chrome azurol S assay and was comparable to that of **2** and deferoxamine (IC_{50} 13.4, 9.5, and 6.3 μM, respectively). Nocardamin glucuronide (**1**) is the first example of a siderophore glucuronide.

In search for new bioactive compounds, the *Streptomyces* sp. 80H647 strain was subjected to the one strain-many compounds (OSMAC) method [1]. This strain is a producer of the nucleoside antibiotic, ascamycin [2], and we hypothesized that the production of more structurally interesting metabolites will be stimulated under different culture conditions [1].

Six different culture media (70 mL) were prepared (Table S1), inoculated, and incubated with shaking at 150 rpm and 28 °C for 5 days. A small-scale extraction was done to obtain EtOAc, BuOH, and aqueous extracts, which were evaporated to dryness. The extracts were subjected to bioactivity screening and LC-MS analysis. MS data were used for the principal component analysis, which presented samples cultured in corn steep liquor-dried yeast (CD) and oatmeal (OA) in separate groups while the rest of the samples were clustered with the blank (Fig. 1). This clearly indicated that there was a difference between the metabolite profiles of the CD and OA cultures while there was no or reduced metabolite production in the other media; hence, confirming the effectiveness of the OSMAC approach. In addition, a volcano plot (*p*-value vs log fold change) of OA samples against all other samples was created and it showed that a compound with *m/z* 777 was unique to OA (Fig. 1). A search of our NPPlot database [3] as well as the Dictionary of Natural Products [4] revealed that it was possibly a new compound and was pursued.

A 2.5-L OA culture was prepared and subjected to liquid–liquid partition, HP20 Diaion resin adsorption, and a number of medium pressure liquid chromatography runs to obtain pure compounds, **1** and **2** (Fig. 2 and S1). Compound **1** was the target compound with *m/z* 777, while **2** was a major metabolite with *m/z* 601. The planar structures were deduced by interpretation of the MS and NMR data. Using high-resolution ESI-TOFMS data (Figs. S2 and S3), the following molecular formula were acquired: $C_{33}H_{56}N_6O_{15}$ for **1** ($[M+H]^+$ *m/z* 777.3887, calcd 777.3876), and $C_{27}H_{48}N_6O_9$ for **2** ($[M+H]^+$ *m/z* 601.3570, calcd 601.3556). Compound **2** had nine signals in its ^{13}C NMR spectrum and seven spin systems plus two exchangeable protons in its ^1H NMR spectrum (Table 1, Fig. S4). Considering its molecular formula, these NMR signals were determined to be three repeating units of *N*-hydroxy-

This article is dedicated to Dr Kiyoshi Isono with respect and admiration for his achievements in antibiotics research.

Supplementary information The online version of this article (https://doi.org/10.1038/s41429-019-0217-5) contains supplementary material, which is available to authorised users.

✉ Hiroyuki Osada
cb-secretary@ml.riken.jp

[1] RIKEN Center for Sustainable Resource Science, Chemical Biology Research Group, 2-1 Hirosawa, Wako, Saitama 351-0198, Japan

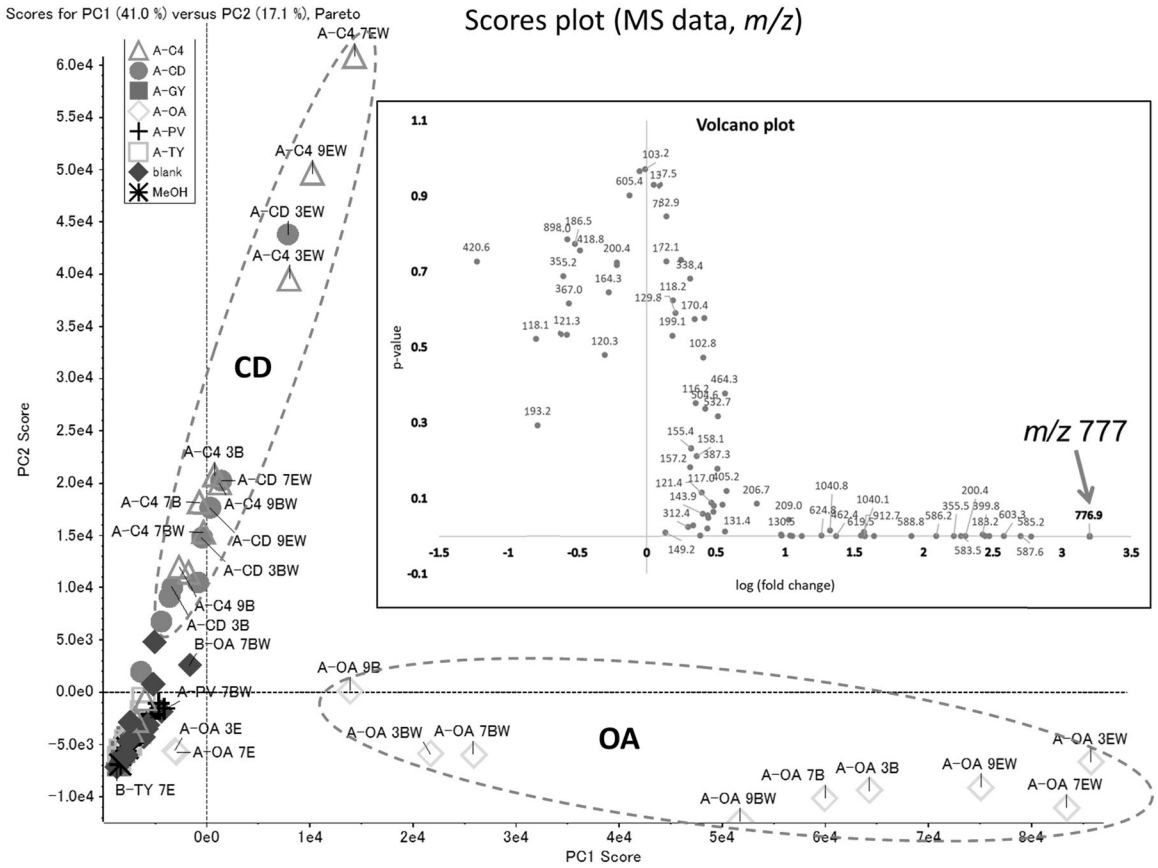

Fig. 1 Principal component analysis of the MS data of *Streptomyces* sp. 80H647 extracts cultured in different media and volcano plot of OA extracts against all other samples. The composition of each medium is listed in Table S1. Blank refers to medium only. The numbers (3, 7, and 9) indicate pH. B and E denotes BuOH and EtOAc extracts, respectively, and W is the corresponding aqueous layer. CD is a modified and updated version of C4. The corresponding volcano plot is shown in the box

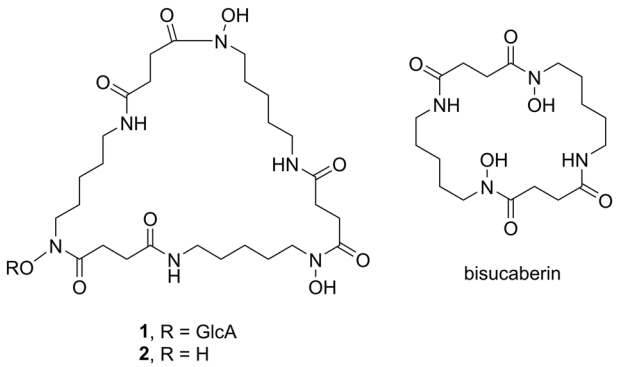

Fig. 2 Structures of nocardamin glucuronide (**1**), nocardamin (**2**), and bisucaberin

N′-succinylcadaverine, which is characteristic of nocardamin, also known as desferrioxamine E [5–7].

Although similar signals for nocardamin were evident in the ^{1}H NMR spectrum of **1**, additional smaller peaks were observed at δ_H 3–5 ppm (Fig. S4). Extra peaks at δ_C 70–80 and 105.7 or 105.1 ppm were also found in the ^{13}C NMR spectrum of **1** (Figs. S7 and S8). DEPT-135 and HSQC data (Figs. S9 and S10) revealed that these signals corresponded to methines. COSY and TOCSY data (Figs. S11 and S12) also showed that they form a separate spin system apart from the methylenes of the nocardamin unit. Based on the chemical shifts of these methines and a mass difference of 176 Da between **1** and **2**, a nocardamin glucuronide structure was proposed for **1** (Fig. 2).

Connections were established by analysis of 2D NMR data (Fig. 3 and S10–S14). The *N*-hydroxy-*N*′-succinylcadaverine assembly was based on the following correlations: COSY signals from H-2 through NH-7, and between H-9 and H-10; TOCSY signals from NH-7 to H-6 and H-5; HMBC from H-2 and H-6 to C-4 (in D_2O), from H-6 (in D_2O) and H-10 to C-8, and from H-2 (in D_2O) and H-9 to C-11. The glucuronic acid (GlcA) moiety was supported by the following data: COSY signals from H-1′ though H-5′, and HMBC from H-5′ to C-1′ and C-6′ (in D_2O). The proposed structure of **1** also satisfies nine degrees of unsaturations as calculated from the molecular formula. Moreover, MS/MS data (Fig. S15) showed fragment ions corresponding to a loss of 176 Da (*m/z* 601) and 200 Da (*m/z* 577; and 401, 201 from 601) consistent with the loss of GlcA and *N*-hydroxy-*N*′-succinylcadaverine, respectively.

Table 1 ^{1}H and ^{13}C NMR data of **1** and **2**

	1[a]		2[a]		Literature (bisucaberin)[b,5]	
Position	δ_H (mult., *J* in Hz)	δ_C	δ_H (mult., *J* in Hz)	δ_C	δ_H (mult., *J* in Hz)	δ_C
1, N-OH	9.88 (br s)		9.6 (br s)		9.53 (s)	
2, CH_2	3.48, 3.69[c] (m)	46.8	3.46 (t, 6.9)	46.8	3.48 (t, 6.3)	46.3
3, CH_2	1.49 (m)	25.9	1.51 (m)	25.8	1.47 (m)	25.5
4, CH_2	1.19 (m)	23.2	1.20 (m)	23.1	1.15 (m)	22.5
5, CH_2	1.36 (m)	28.6	1.37 (m)	28.6	1.35 (m)	28.2
6, CH_2	2.99 (m)	38.3	3.00 (m)	38.3	3.01 (br m)	37.9
7, NH	7.75 (br t)		7.72 (br t)		7.61 (br t)	
8, C=O		171.9		172.0		171.8
9, CH_2	2.27 (m)	30.2	2.28 (t, 6.3)	30.0	2.27 (t, 7.4)	30.5
10, CH_2	2.58, 2.86[c] (m)	27.7	2.58 (m)	27.5	2.57 (t, 7.4)	27.8
11, C=O		171.5		171.4		171.5
					literature (GlcA part)[f,8]	
1′, CH	4.62 (d, 8.0)	105.7[d]			4.57 (d, 8.5)	105.7
2′, CH	3.08 (m)	71.8			3.04 (m)	72.2
2′-OH	5.38 (br d)					
3′, CH	3.22 (m)	76.4			3.22 (m)	76.6
3′-OH	5.1 (br s)					
4′, CH	3.22 (m)	71.7			3.33 (m)	72.0
4′-OH	5.1 (br s)					
5′, CH	3.44 (m)	74.4			3.65 (m)	75.9
6′, COOH		173.1[e]				171.3

[a]500 MHz for ^{1}H, 125 MHz for ^{13}C, DMSO-d_6

[b]400 MHz for ^{1}H, 100 MHz for ^{13}C, DMSO-d_6

[c]Signals affected by GlcA

[d]From HSQC data, DMSO-d_6

[e]From HMBC data, D_2O

[f]500 MHz for ^{1}H, 125 MHz for ^{13}C, D_2O/CD_3CN/DMSO-d_6 (2/3.5/6)

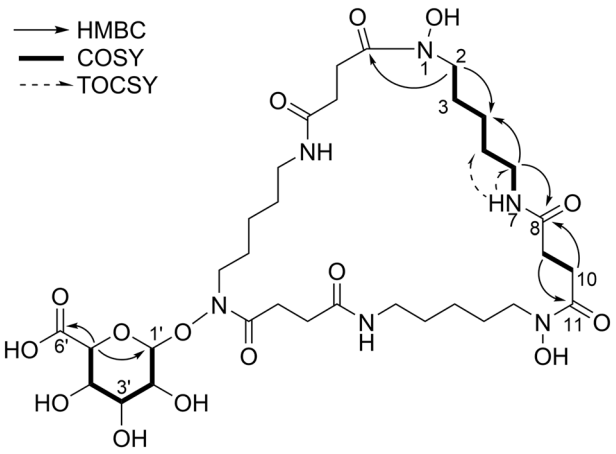

Fig. 3 Key 2D NMR data of **1**

The chemical shifts observed for GlcA (Table 1) and its observed cleavage from the macrolide during fragmentation is in agreement with other reported *N*-*O*-glucuronides [8]. In addition, the possibility of an N^{+} glucuronide was eliminated on the basis of the chemical shift values on GlcA and the weak downfield shifts on the γ (H-2) and δ (H-10) positions from GlcA in comparison with the literature [8]. Unlike in **2**, H-2 and H-10 showed nonequivalent protons in **1** as seen in the HSQC spectrum (Fig. S10) indicating asymmetry caused by the presence of GlcA. Likewise, paired ^{13}C NMR signals (C-3, C-5, C-9, and C-10, Fig. S7) were detected, which were not present in **2**. The occurrence of nonequivalent protons (H-2 and H-10) in **1** confirmed the placement of GlcA on the hydroxamic acid group rather than the amide nitrogen.

To determine the absolute configuration of GlcA, hydrolysis, derivatization, and subsequent comparison with standards were performed. To accomplish this, GlcA was obtained by using β-glucuronidase (Fig. S16). The successful enzymatic cleavage of GlcA suggested a β configuration of the anomeric carbon which was also supported by chemical shift (δ_C 105.7, δ_H 4.62) and coupling constant data ($J = 8.0$ Hz) [8]. Furthermore, a D configuration was predicted since D-glycosides are usually in the β form [9].

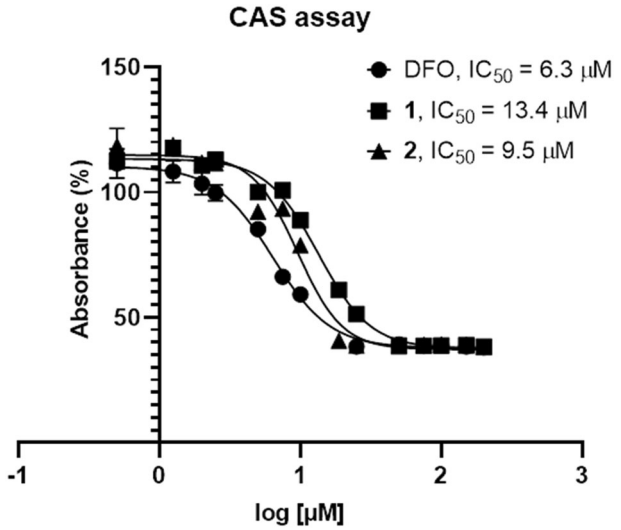

Fig. 4 Dose-response curve of the siderophore activity **1**, **2**, and deferoxamine (DFO)

To confirm this, the hydrolysate and standards, D- and L-GlcA, were separately reacted with L-cysteine methyl ester followed by phenylisothiocyanate according to the method of Tanaka et al. [10]. The derivatives were analysed by LC-MS and results showed that the mass and retention time of the sample matched that of D-GlcA (Fig. S17). Thus, GlcA was unambiguously determined to have the β-D configuration.

Since nocardamin (**2**) is a known siderophore [7], the iron binding activity of **1** was evaluated via the chrome azurol S assay [11]. Indeed, **1** exhibited iron chelating properties comparable to **2** and deferoxamine (DFO or desferrioxamine B) at IC_{50} 13.4, 9.5, and 6.6 µM, respectively (Fig. 4). On the other hand, the cytotoxicity test of **1** and **2** at 39 and 50 µM, respectively, was negative against the following cell lines: HeLa (cervical cancer), HL-60 (leukaemia), MKN-74 (gastric cancer), MG-63 (osteosarcoma), MIA PaCa-2 (pancreatic cancer), SK-MEL-28 (melanoma), and T98G (glioblastoma). At the same concentrations, compounds **1** and **2** did not induce differentiation of C3H10T1/2 mesenchymal stem cells and did not inhibit the growth of *Aspergillus fumigatus* Af293, *Escherichia coli* HO141, *Pyricularia oryzae* kita-1, and *Staphylococcus aureus* 209. In addition, compound **2** showed mild antimalarial activity (IC_{50} 10 µM), while **1** was inactive suggesting that glucuronidation altered the activity. The GlcA moiety makes **1** less lipophilic than **2**, which may indicate that **2** can pass the cell membrane more easily delivering its antimalarial effect more effectively [12]. To support this, logP values were calculated by using MayaChemTools [13]. The calculated logP values for DFO, **1**, the carboxylate form of **1**, and **2** (3.14, 1.77, 0.44, and 3.07, respectively) demonstrated the more lipophilic property of **2** over **1**.

To our knowledge, nocardamin glucuronide (**1**) is the first example of a siderophore glucuronide. Glucuronides play an important role in drug metabolism and pharmacokinetics [14], such as detoxification and enterohepatic recirculation, although majority of the studies are focused on the mammalian system. In addition, there are only few reports on the production of glucuronides by microbial enzymes [12] and little is known about their function and biosynthesis. Though a minute amount of nocardamin (**2**) was also found in the CD culture, the production of **1** and **2** were particularly enhanced in the OA medium. While a possible explanation for this outcome could not be supposed, it shows that OSMAC is an efficient way of stimulating cryptic and variable secondary metabolism. On the other hand, siderophores continue to be a hot topic in the areas of antibiotics, drug conjugates, drug resistance, and combination therapy for the treatment of various illnesses such as infections, cancer, and neurodegenerative diseases [15–17].

Acknowledgements This work was supported in part by JSPS KAKENHI Grant Numbers JP16H06276, JP17H06412, and JP18H03945. We would like to thank Ms Harumi Aono, Ms Akiko Okano, Dr Rachael Uson-Lopez, Ms Emiko Sanada, and Dr Motoko Uchida for technical support.

Compliance with ethical standards

Conflict of interest The authors declare that they have no conflict of interest.

Publisher's note: Springer Nature remains neutral with regard to jurisdictional claims in published maps and institutional affiliations.

References

1. Bode HB, Bethe B, Hofs R, Zeeck A. Big effects from small changes: possible ways to explore nature's chemical diversity. ChemBioChem. 2002;3:619–27.
2. Isono K, et al. Ascamycin and dealanylascamycin, nucleoside antibiotics from *Streptomyces* sp. J Antibiot. 1984;37:670–2.
3. Lim CL, Nogawa T, Uramoto M, Okano A, Hongo Y. RK-1355A and B, Novel quinomycin derivatives isolated from a microbial metabolites fraction library based on NPPlot screening. J Antibiot. 2014;67:323–9.
4. CRC Press. Dictionary of Natural Products. (2018) http://dnp.chemnetbase.com. Accessed 5 Mar 2018.
5. Takahashi A, et al. Bisucaberin, a new siderophore, sensitizing tumor cells to macrophage-mediated cytolysis. J Antibiot. 1987;40:1671–6.
6. Ueki M, et al. Nocardamin Production by *Streptomyces avermitilis*. Actinomycetologica. 2009;23:34–9.
7. Hossain MB, van der Helm D, Poling M. The structure of deferriferrioxamine E (Nocardamin), a cyclic trihydroxamate. Acta Cryst B. 1983;39:258–63.
8. Uldam HK, Juhl M, Pedersen H, Dalgaard L. Biosynthesis and identification of an N-Oxide/N-Glucuronide metabolite and first

synthesis of an N-O-glucuronide metabolite of Lu AA21004. Drug Metab Dispos. 2011;39:2264–74.
9. Klyne W. The configuration of the anomeric carbon atoms in some cardiac glycosides. Biochem J. 1950;47:xli–ii.
10. Tanaka T, Nakashima T, Ueda T, Tomii K, Kouno I. Facile discrimination of aldose enantiomers by reversed-phase HPLC. Chem Pharm Bull. 2007;55:899–901.
11. Lopez JAV, et al. Wewakazole B, a cytotoxic cyanobactin from the cyanobacterium *Moorea producens* collected in the Red Sea. J Nat Prod. 2016;79:1213–8.
12. Docampo M, Olubu A, Wang X, Pasinetti G, Dixon RA. Glucuronidated flavonoids in neurological protection: structural analysis and approaches for chemical and biological synthesis. J Agr Food Chem. 2017;65:7607–23.
13. Sud M. MayaChemTools: an open source package for computational drug discovery. J Chem Inf Model. 2016;56:2292–7.
14. Stachulski AV, Meng X. Glucuronides from metabolites to medicines: a survey of the in vivo generation, chemical synthesis and properties of glucuronides. Nat Prod Rep. 2013;30:806–48.
15. Wilson BR, Bogdan AR, Miyazawa M, Hashimoto K, Tsuji Y. Siderophores in iron metabolism: from mechanism to therapy potential. Trends Mol Med. 2016;22:1077–90.
16. Hider RC, Roy S, Ma YM, Le Kong X, Preston J. The Potential application of iron chelators for the treatment of neurodegenerative diseases. Metallomics. 2011;3:239–49.
17. Schalk IJ, Mislin GLA. Bacterial Iron uptake pathways: gates for the import of bactericide compounds. J Med Chem. 2017;60:4573–6.